

*Article*

## Liquid-Phase Exfoliation of Graphite Using the Serum from Skim Natural Rubber Latex

Natchanon Jirasitthanit<sup>a</sup> and Panu Danwanichakul<sup>b,\*</sup>

Department of Chemical Engineering, Faculty of Engineering, Thammasat School of Engineering, Thammasat University, Pathum Thani 12120, Thailand

E-mail: <sup>a</sup>nat.cha.non@hotmail.com, <sup>b,\*</sup>dpanu@engr.tu.ac.th (Corresponding author)

**Abstract.** The green exfoliation of graphite by using the serum from skim natural rubber latex together with ultrasonication was investigated. The rubber particles were coagulated with 0.7% w/v cationic polyacrylamides solution and the remaining serum containing ammonia was used as an exfoliating medium. The suspension with 25 mg graphite/ml serum was sonicated for 2 h at 29-53°C in an ultrasonic bath at 40 kHz and was left standing for 2 h at room temperature. The top part was centrifuged at 2000 rpm for 30 min and then the top section of this was centrifuged at 10500 rpm for 30 min to collect the solid. This process was repeated 2-3 times using the bottom part of the sedimentation. The yield of exfoliated graphite sample from each exfoliation process ranged from 0.20-0.35% and showed quality of multilayer graphene based on Raman spectroscopy results, which was comparable to the commercial graphene. The samples were also checked with scanning electron microscope and underwent some experiments, including sedimentation and methylene blue adsorption. It was found that the high-quality exfoliated sample showed better dispersion in water, resulting in 99% turbidity after 20-min sedimentation and yielded higher adsorption capacity than that of the commercial graphene.

**Keywords:** Liquid-phase exfoliation, ammonia, skim natural rubber latex, graphite, graphene.

**ENGINEERING JOURNAL** Volume 27 Issue 5

Received 15 October 2022

Accepted 20 May 2023

Published 31 May 2023

Online at <https://engj.org/>

DOI:10.4186/ej.2023.27.5.37

## 1. Introduction

Skim natural rubber latex (SNRL) is a by-product in the concentrated latex production. Fresh natural rubber latex (FNRL) contains colloids of rubber particles which are composed of cis-1,4-polyisoprene as the rubber core covered by some proteins and phospholipids. After tapping, FNRL coagulates and rots rapidly so ammonia (NH<sub>3</sub>) was added to prevent bacteria attack and increase colloidal stability. After centrifugation of FNRL, the concentrated latex containing approximately 60% dry rubber content (DRC) is obtained along with SNRL containing 4-7% DRC and residual ammonia [1]. SNRL is a low-cost by-product or waste in some smaller factories. The treatment of SNRL typically begins with coagulation of the rubber particles using sulfuric acid (H<sub>2</sub>SO<sub>4</sub>) solution at a high concentration yielding a rubber coagulum which is made into low-quality skim block and skim crepe and a large volume of liquid which is called serum.

Recently, there have been many researches focusing on new applications of SNRL. For example, the films of deproteinized skim natural rubber have been studied to be used as a controlling layer in the permeation of salicylic acid, which showed a good potential in medical purposes [2]. The serum obtained after acid coagulation contains a lot of organic materials including L-quebrachitol, which is a starting material for drugs to treat diabetes and cancer. A process including ion exchanges, adsorption, solvent extractions and drying, has been proposed to obtain L-quebrachitol from the highly acidic serum [3].

The treatment of SNRL using sulfuric acid is not environmentally friendly so new coagulating media for rubber coagulation were investigated including chitosan in acetic acid and cationic polyacrylamide (PAM<sup>+</sup>) solutions. The treatment yielded better properties of waste water and higher quality skim rubber [4]. In case of using PAM<sup>+</sup>, the remaining serum still contains ammonia which could be useful. Organic substances including sugars, fatty acids and proteins as well as the left-over ammonia in the serum could be of use as reducing and stabilizing agents in the synthesis of metallic nanoparticles such as silver and gold nanoparticles [5-7].

Not only metallic nanoparticles have been of great interest in a wide range of applications in consumer goods to medical products but other nanomaterials including graphene have also been the focus in material science and engineering. Graphene is a 2D material composed of carbon atoms connecting with covalent bonds in a hexagonal structure. It has many outstanding properties including high strength, light-weight, high toughness, very good electrical and thermal properties at room temperature. Therefore, graphene composites are used as sport equipment, a bending touch screen, electrodes in batteries, and drug delivery materials [8]. Graphene synthesis can be classified into two large types: bottom-up

method, in which the molecules of carbon atoms from a carbon source are arranged to form graphene, such as pyrolysis, chemical vapor coating, etc., and top-down method, in which graphite layers held together by weak van der Waal's forces are separated, such as mechanical and chemical exfoliation [8]. The most commonly used top-down method is the Hummer method, in which a strong acid was used as an oxidizing agent to turn graphene to graphene oxide (GO) which could be more exfoliated and dispersed in water but was lower in electrical conductivity. Therefore, a reducing agent may be used to convert graphene oxide to reduced graphene oxide (rGO) [9-15]. However, in the above method, many hazardous chemicals and large amounts of water were used. In addition, the obtained graphene was defected and sometimes contaminated with residual chemicals. In addition, for the application involved electrical conductivity of graphene, the properties closely rely on the extent of the reduction of graphene oxide.

To avoid the uses of dangerous chemicals and large amounts of water, and keep the electrical properties intact as much as possible, exfoliations of graphite in the liquid phase using various substances were investigated. For example, one research studied the exfoliation of graphite using 5.0 g graphite powder in 500.0 mL N-methyl-2-pyrrolidone (NMP) (10 mg/ml) and then sonication (100W, 40 kHz) for 48 h. It was found that the graphene yield was 0.2% and it was then used to construct an electrochemical sensor for highly-sensitive detection of diethylstilbestrol and estradiol [16].

In another work, the direct exfoliation of graphite to obtain few-layer graphene using N-methyl-2-pyrrolidone (NMP) together with Fe<sub>3</sub>O<sub>4</sub> nanoparticles in combination with ultra-sonication at the power of 240 – 600 W for 30–120 min was studied. It was found that using NMP at the initial concentration of 0.5 mg graphite/mL NMP gave the highest exfoliation yield of 19%. If together with the use of ultra-sonication for 90 min, the yield could be increased to 20%. The presence of Fe<sub>3</sub>O<sub>4</sub> nanoparticles also increased the exfoliation efficiency [17].

In addition, the efficiency improvement of the exfoliation was done by using the combination of NMP and organic salts such as sodium citrate, sodium tartrate, and potassium citrate. It was found that the exfoliation of 10 mg graphite in 1 ml NMP with K-Citrate resulted in a graphene yield of 10% and up to 50% after 8 cycles of exfoliation. [18].

Among the green solvents which were inexpensive and less toxic in the exfoliation of graphite, water is the most interesting substance. It has been proposed to use water with different organic surfactants or use an alkaline aqueous solution together with the use of ultra-sonication at high and low frequency (1174 kHz and 20 kHz) to obtain a suspension of monolayer or a few layers. The results showed a 10% graphene yield [19].

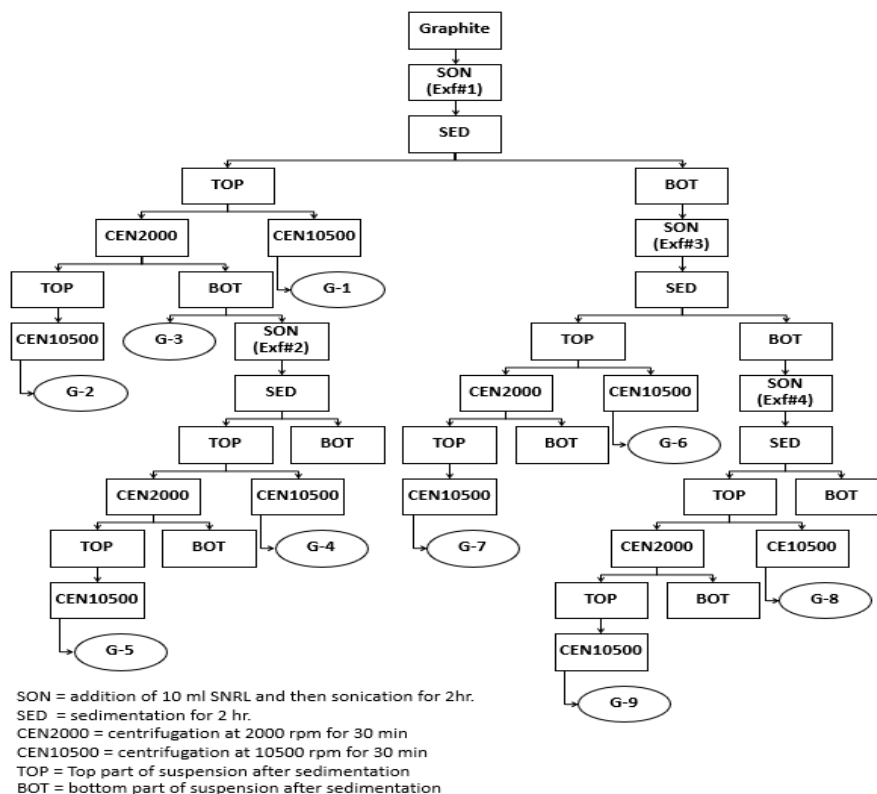


Fig. 1. The scheme of multi-exfoliation of graphite to yield various exfoliated graphite samples (G-1 to G-9).

In other works, it was found that ammonia or urea could play an important role in exfoliating graphite in purified water, resulting in a high-quality graphene sheet and graphene yield of 0.29% [20] and 0.12% [21], respectively. As explained earlier, the left-over ammonia still remains in the serum after the treatment of SNRL with cationic polyacrylamide solution. Therefore, it could be useful in the exfoliation of graphite so the preliminary experiment was done and it was confirmed that by following the method in [20], ammonia in the serum was effective and resulted in a similar graphene yield of 0.28% [22].

The rubber industry is one of the most important industries of Thailand. The production of concentrated latex was reported as high as 964,403 tons in 2015 [23], which could yield about 1,155,355 tons of SNR. Therefore, the serum of SNRL could be a sustainable source for nanomaterial industries of which the exfoliation of graphite is a focus in this current study. This research, thus, extended our previous preliminary study and aimed to investigate the multi-step exfoliation of graphite by using the serum from SNRL with ultra-sonication to increase the overall yield of the graphene production. It is also interesting to study how each step affected the properties of its products so the Raman spectroscopy results would be compared. In addition, the comparisons were also made with the graphite precursor and the commercial graphene.

Not only the Raman spectroscopy and scanning electron microscopy were applied but certain experiments including sedimentation and adsorption using exfoliated graphite products were investigated together with the precursor graphite and the commercial graphene.

## 2. Experimental

### 2.1. Raw Materials

Extra pure fine powder graphite (the particle size less than 50  $\mu\text{m}$ ) was purchased from Merck & co. inc. Skim natural rubber latex (SNRL) was provided by Thai Eastern Group Holdings Public Co.,Ltd. (Thailand). Cationic polyacrylamide (PAM<sup>+</sup>) was supplied by Welkin Enterprise Co.,Ltd. (Thailand). Sodium dodecyl sulfate (SDS) and methylene blue (MB) were purchased from Ajax Finechem. The commercial graphene was provided by TCI (the thickness of 6-8 nm and the width of 5  $\mu\text{m}$ ).

### 2.2. Preparation of the Serum from Skim Natural Rubber Latex

To coagulate the rubber particles in the SNRL, 200 ml of 0.7% w/v PAM<sup>+</sup> solution was added to 250 ml of SNRL and the mixture was stirred at a low speed of 200 rpm to mix the suspension. The rubber particles were coagulated and the coagulum could be removed. After that the liquid was filtered with a piece of nylon fabric and the

clear yellowish liquid was obtained which is called the serum. The pH of the serum was measured.

### 2.3. Liquid Phase Exfoliation of Graphite

The scheme of multi-step exfoliation of graphite using the serum from SNRL as an exfoliating medium was shown in Fig. 1. Initially, the graphite concentration at 25 mg/ml was prepared by mixing 250 mg graphite powder with 10 ml serum from SNRL. The mixture was sonicated for 2 h at 29-53°C in an ultrasonic bath (200 W, 40 kHz) and was left to stand for 2 h at room temperature for the sedimentation to occur. This is called one step of exfoliation (Exf#1). The top and bottom parts were to be processed further.

The top part from Exf#1 was either centrifuged at 10500 rpm for 30 min to collect the sample called G-1 or centrifuged at 2000 rpm for 30 min and separated into top and bottom sections. The top section was then centrifuged to obtain the sample called G-2 while the bottom section underwent the next step of exfoliation (Exf#2) by adding 10 ml of the serum which followed by sonication for 2 h and sedimentation for 2 h. The top part from Exf#2 was processed either by centrifugation at 10500 for 30 min to yield sample G-4 or by centrifugation at 2000 rpm, for 30 min followed by the separation to top and bottom suspensions of which the top one was centrifuged to obtain sample called G-5.

The bottom part from Exf#1 was exfoliated one more time (Exf#3) by sonication and sedimentation to yield the top and bottom parts. The top part from Exf#3 was either centrifuged at 10500 rpm for 30 min to collect the sample called G-6 or centrifuged at 2000 rpm for 30 min to separate the top and bottom sections, of which the top one was collected as the sample called G-7. The bottom part from Exf#3 was further exfoliated (Exf#4) via sonication and sedimentation and the top part underwent either centrifugation at 10500 rpm for 30 min to obtain sample called G-8 or centrifugation at 2000 rpm for 30 min, after that the top part was collected as sample called G-9.

Each collected sample was washed with 1%wt/vol sodium dodecyl sulfate (SDS) solution and later with distilled water and it was dried in an oven at 80°C until the weight was constant. The yield percentage of each sample could be defined as

$$\% \text{ yield} = \frac{\text{mass of the exfoliated graphite sample}}{\text{mass of the precursor graphite}} \times 100 \quad (1)$$

### 2.4. Characterization of the Exfoliated Graphite Samples

#### 2.4.1. Raman Spectroscopy

Raman spectroscopy results of all the exfoliated graphite samples (G-1 to G-9) were obtained using a dispersive Raman microscope (Bruker Optics, Model:

Senterra) with laser wavelength at 532 nm (the laser power of 5 mW and the spectral range of 4500 - 70  $\text{cm}^{-1}$ ). The measurement followed the standard methods, ASTM: E1693 and ASTM: E1840.

#### 2.4.2. Scanning electron microscopy

The structures and surface morphology of some chosen exfoliated graphite samples were investigated using a scanning electron microscope (SEM, JSM-7800F) with an accelerating voltage of 15 kV. The magnification was adjusted to 20000X.

### 2.5. Sedimentation Experiment

Each of the chosen exfoliated graphite samples weighing about 0.005 g was dispersed in 1.5 ml of 1%wt/vol SDS solution and the mixture was mixed homogeneously using the vortex mixer for 30 s. and then pipetted into a cuvette. The sedimentation of each sample was studied by measuring the absorbance of the settling sample using UV-vis spectroscopy (METASH, Model V-5100 /UV5100) at various times in the period of 20 min. The spectral range was between 330 and 600 nm.

With the absorbance values in the whole spectral range, the average absorbance value could be determined by Eq. (2).

$$A_{ave} = \frac{\int_{330}^{600} A(\lambda) d\lambda}{\int_{330}^{600} d\lambda} \quad (2)$$

The turbidity percentage (%T) and the absorbance value of the sample are closely related as shown in Eq. (3).

$$A_{av} = 2 - \log_{10}(\%T) \quad (3)$$

Then, the turbidity percentage at various times during the sedimentation period could be determined for each sample.

### 2.6. Adsorption Experiment

#### 2.6.1. Preparation of the calibration curve of methylene blue solution

The adsorption experiments of the chosen exfoliated graphite samples were performed by using methylene blue (MB) as the adsorbate. Therefore, the linear calibration curve of MB in water was prepared for the solutions with the concentration of 1.25, 2.5, 3, 5 and 9 ppm. Each was measured for the absorbance at 665 nm using UV-vis spectroscopy. The correlation had to yield the value of  $R^2$  greater than 0.99.

## 2.6.2. Absorption experiment

Each of the chosen exfoliated samples weighing 0.005 g was added into a vessel containing 45 ml methylene blue (MB) solution at different concentration of 1.25, 2.5, 3, 5 and 9 ppm. After that, it was mixed by the vortex mixer for 30 s at room temperature (25°C). The mixtures were then shaken in an orbital shaker at 150 rpm for 2 h, during which the liquid was sampled every 10 min to check for the absorbance using UV-vis spectroscopy. The concentration of the MB solution was then calculated using the prepared calibration curve.

The ability to remove MB may be expressed in terms of the adsorption percentage, defined in Eq. (4) [24-27].

$$\text{Adsorption percentage} = \frac{(C_o - C_t)}{C_o} \times 100 \quad (4)$$

where  $C_o$  and  $C_t$  are the initial concentration (mg/l) and the concentration (mg/l) of MB at any adsorption time,  $t$ , respectively. The adsorption capacity at any time,  $q_t$  is defined as shown in Eq. (5),

$$q_t = \frac{(C_o - C_t)V}{m} \quad (5)$$

where  $q_t$  is the adsorption capacity at any time (mg MB/g sample),  $V$  is the volume of MB solution (l) and  $m$  is the mass of the exfoliated graphite sample (g).

To study the adsorption kinetics, the pseudo-first-order and pseudo-second-order kinetic models could be used [24-27]. The pseudo-first-order kinetics equation is expressed as

$$\frac{dq_t}{dt} = k_1(q_e - q_t) \quad (6)$$

where  $q_t$  and  $q_e$  are the adsorption capacity (mg MB/g sample) at any time  $t$  and at equilibrium, respectively. The parameter  $k_1$  is the Lagergren rate constant of the pseudo-first-order adsorption ( $\text{min}^{-1}$ ). Upon integration of Eq. (6) using the initial condition,  $q_t(0) = 0$ , and condition at any time  $t$ ,  $q_t(t) = q_t$ , Eq. (7) was obtained.

$$\ln(q_e - q_t) = \ln(q_e) - k_1 t \quad (7)$$

When  $\ln(q_e - q_t)$  is plotted against  $t$ , the slope and the intercept of the plot could be used to determine the rate constant  $k_1$  and  $q_e$ , respectively [24-27].

The equation of the pseudo-second-order is expressed as

$$\frac{dq_t}{dt} = k_2(q_e - q_t)^2 \quad (8)$$

where the variables are defined the same and the parameter  $k_2$  is the rate constant of the pseudo-second-

order adsorption ( $\text{g mg}^{-1} \text{min}^{-1}$ ). With the initial condition of  $q_t(0) = 0$ , and that of any time  $q_t(t) = q_t$ , Eq. (8) is integrated to yield Eq. (9).

$$\frac{t}{q_t} = \frac{1}{k_2 q_e^2} + \frac{1}{q_e} t \quad (9)$$

The plot of the linearized equation, Eq. (9), of  $t/q_t$  versus  $t$  yields  $q_e$  and  $k_2$  from the slope and the intercept, respectively [24-27].

Because adsorption is one of the processes that could reach an equilibrium point where at a constant temperature the chemical potential of the adsorbate on the solid surface is the same as that in the liquid phase. To study the adsorption equilibrium, two basic models, Langmuir and Freundlich isotherms, are usually applied. Langmuir adsorption isotherm describes monolayer adsorption of the substance on the surface of the adsorbent so the maximum adsorption capacity ( $q_{\text{max}}$ ) on the adsorbent surface could be approximated. The Langmuir isotherm equation in a linearized form is expressed in Eq. (10).

$$\frac{1}{q_e} = \left( \frac{1}{q_{\text{max}} K_L} \right) \frac{1}{C_e} + \frac{1}{q_{\text{max}}} \quad (10)$$

where  $q_e$  and  $q_{\text{max}}$  are the equilibrium adsorption capacity (mg/g) and the maximum adsorption capacity of the adsorbent (mg/g), respectively.  $C_e$  is the equilibrium concentration of MB in the solution (mg/L) and  $K_L$  is the Langmuir isotherm constant (L/mg) which is related to the free energy of adsorption. The plot of  $1/q_e$  against  $1/C_e$  could be prepared and the slope along with the intercept are obtained to determine both  $q_{\text{max}}$  and  $K_L$  [24-27].

While Langmuir isotherm best describes the monolayer adsorption, Freundlich isotherm could be applied to explain the multi-layer absorption where adsorbate molecules could be on top of one another. The isotherm is expressed in a linearized form in Eq. (11).

$$\ln q_e = \frac{1}{n} \ln C_e + \ln K_F \quad (11)$$

Here, Freundlich parameters  $K_F$  and  $n$  are obtained when  $\ln q_e$  is plotted versus  $\ln C_e$ . The values of  $n$  and  $K_F$  are obtained from the slope and intercept, respectively [24-27].

## 3. Results and Discussion

### 3.1. The Yields of the Exfoliated Graphite Samples

Various exfoliated graphite samples (G-1 to G-9) were collected from the multi-step exfoliation process (Exf#1, Exf#2, Exf#3 and Exf#4) using the serum from SNRL of which the pH was 8.91-9.12, together with the ultra-

sonication as described in Section 2.3 and shown in Fig. 1. The yield percentages of all samples were displayed in Table 1.

Table 1. %Yield of the exfoliated graphite samples.

Sample	%Yield
G-1	4.18
G-2	0.32
G-3	3.94
G-4	1.00
G-5	0.20
G-6	0.68
G-7	0.24
G-8	1.28
G-9	0.35

The samples G-1 and G-2 were the exfoliated products from the step Exf#1, G-4 and G-5 from Exf#2, G-6 and G-7 from Exf#3, and G-8 and G-9 from Exf#4. All reported yields were small when compared with using other NMP solvents with the amounts of graphite used was much lower, 10 and 0.5 mg/ml [16, 17]. But our result (the yield of G-2) was consistent with the one reported in the literature using ammonia at pH ~9 [20], confirming the effect of remaining ammonia in the serum of SNRL. For every pair, collecting of top part products after centrifugation at 2000 rpm gave smaller yields than those collecting all particles after centrifugation at 10500 rpm.

Obviously, more steps of exfoliation (adding the serum and further sonication) could increase the overall yields of exfoliated graphite. However, the quality of exfoliated graphite products had to be checked with Raman spectroscopy results which would be discussed in the next section.

### 3.2. Characterization of the Exfoliated Graphite Samples

#### 3.2.1. Raman spectroscopy results

The characteristics of the exfoliated graphite samples (G-1 to G-9) along with the precursor graphite and the commercial graphene were analyzed through Raman scattering because it was very sensitive to crystal defects and the number of layers in graphene sheets. Typically, three major peaks are detected, the D peak at  $\sim 1350\text{ cm}^{-1}$ , the G peak at  $\sim 1576\text{ cm}^{-1}$ , and the 2D peak at  $\sim 2700\text{ cm}^{-1}$ . The results of the peak position and intensity of Raman spectra were shown in Fig. 2, and the numbers were tabulated in Table 2 for clarity. A higher D peak represents more defect of the edges. A higher G peak represents more C-C stretching mode in  $\text{sp}^2$  hybridized carbon bonds in the graphene or graphite lattice [28].

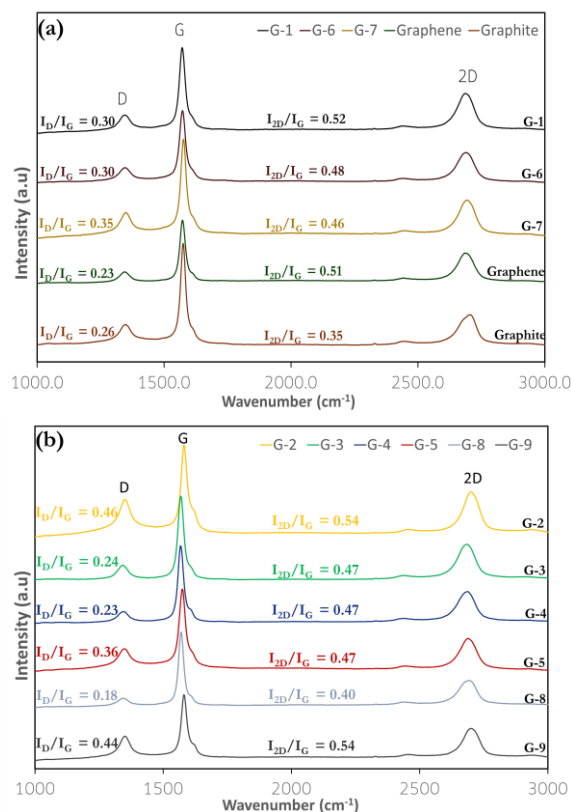


Fig. 2. Raman spectra of all samples were compared where (a) G-1, G-6, G-7, the precursor graphite and the commercial graphene and (b) G-2, G-3, G-4, G-5, G-8, and G-9 were shown.

The shape and the position of the 2D peak is generated by the electron scattering by two phonons [28].

Typically, the D band ( $1350\text{ cm}^{-1}$ ) is sensitive to the structural defects in the graphene and the intensity ratio of the D band to the G band is commonly used to estimate the degree of structural defects in the graphene [20]. The ratio of  $I_{\text{D}}/I_{\text{G}}$  increased after exfoliation value suggested that the ultrasonication induced exfoliation process produced few structural defects on the basal plane of the resultant exfoliated graphite [20, 29].

To investigate the quality of the exfoliated graphite samples, the intensity ratios of two peaks of all samples were compared with those of the precursor graphite and the commercial graphene. It was suggested that the ratios of  $I_{2\text{D}}/I_{\text{G}}$  of graphite, multilayer graphene and bilayer graphene were 0.35, 0.50 and 0.69, respectively [29]. For the precursor graphite, the ratio was 0.35 close to what was reported. All ratios of exfoliated samples were greater than that of graphite and comparable to that of the commercial graphene. They should be of the quality of multilayer graphene [29].

Usually, the ratio  $I_{2\text{D}}/I_{\text{G}}$  decreased with an increase in the number of layers. The exfoliation did not seem to be more effective at later step of exfoliation as the ratio  $I_{2\text{D}}/I_{\text{G}}$  of the samples did not increase. We also did the experiment in which the sonication time was prolonged up to 6 h, instead of 2 h, which might be equivalent to undergoing more steps of exfoliation, the product did not yield higher value of  $I_{2\text{D}}/I_{\text{G}}$ .

Table 2. Results from Raman spectra including peak position, intensity, and the corresponding ratio of all samples.

Sample	D peak (cm <sup>-1</sup> )	D Intensity	G peak (cm <sup>-1</sup> )	G Intensity	2D peak (cm <sup>-1</sup> )	2D Intensity	I <sub>D</sub> /I <sub>G</sub>	I <sub>2D</sub> /I <sub>G</sub>
G-1	1346.03	3274.90	1571.45	11001.68	2686.94	5756.38	0.30	0.52
G-2	1350.56	5451.81	1581.28	11792.02	2699.16	6324.98	0.46	0.54
G-3	1342.15	2570.00	1568.63	10607.49	2684.74	5011.79	0.24	0.47
G-4	1345.88	2345.93	1568.31	10019.35	2687.44	4690.04	0.23	0.47
G-5	1348.43	4005.42	1574.54	10974.33	2688.85	5210.02	0.36	0.47
G-6	1346.03	2748.70	1572.61	9283.91	2688.73	4481.44	0.30	0.48
G-7	1349.82	4604.32	1576.77	13016.12	2693.87	6036.62	0.35	0.46
G-8	1343.50	1719.08	1569.5	9463.99	2692.00	3817.14	0.18	0.40
G-9	1350.50	3798.04	1581.00	8643.22	2701.00	4703.96	0.44	0.54
Graphene	1344.19	1816.98	1572.91	7739.22	2686.20	3967.59	0.23	0.51
Graphite	1347.76	3265.15	1575.10	12580.12	2705.96	4404.66	0.26	0.35

The Raman spectroscopy results were considered in choosing the samples for further investigation via SEM and other experiments. The ratio intensities of I<sub>2D</sub>/I<sub>G</sub> of the samples G-1, G-6 and G-7 were 0.53, 0.49 and 0.46, respectively. These samples were chosen to be studied further via SEM and other experiments along with the graphite precursor and the commercial graphene with the ratios of 0.35 and 0.50, respectively. It would be of interest to see whether the quality level of the obtained exfoliated graphite product based on I<sub>2D</sub>/I<sub>G</sub> affected the results in the sedimentation and adsorption experiments as discussed in Section 3.2.3 and 3.2.4, respectively.

### 3.2.2. Morphology of the exfoliated graphite samples from scanning electron microscope (SEM)

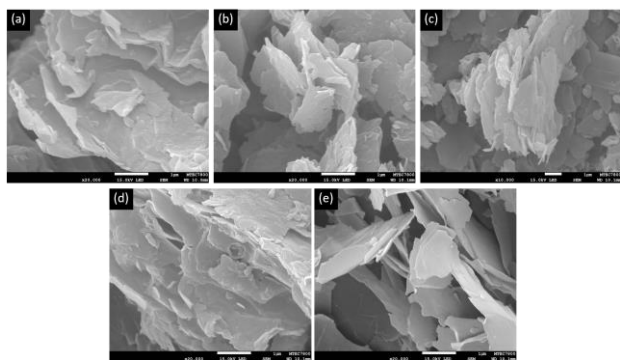


Fig. 3. SEM images of the exfoliated graphite samples, (a) G-1, (b) G-6, (c) G-7, (d) the precursor graphite and (e) the commercial graphene.

The morphology of the chosen exfoliated graphite samples was observed through the micrographs in Fig. 3. The micrographs showed sheets of dispersed exfoliated graphite. Some displayed stacked layers with thin edges. It seemed that the sheets of G-6, G-7 and graphene were smaller than graphite and G-1 probably

because more steps of exfoliation caused breaking up of the sheets.

No impurities were observed, confirming the effective washing twice, once with 1%wt/vol SDS solution and another with water. Fewer layers were seen after exfoliation, assuring the use of residual ammonia from the SNRL with ultra-sonication to successfully exfoliate the graphite. This is consistent with previous result where a small amount of ammonia solution is used to exfoliate graphite [20]. Ammonia was believed to penetrate between the graphite layers, thereby reducing the attraction between the layers and causing exfoliation

The structures of the obtained products were similar to that of the commercial graphene. It can be seen from Fig. 3(a), Fig. 3(b) and Fig. 3(c) that the fracture of the sheets may be caused by sonication and heating corresponding to the ratio I<sub>D</sub>/I<sub>G</sub> values in Table 2. The higher value of the ratio I<sub>D</sub>/I<sub>G</sub> indicated more damages on basal planes caused by the ultrasonication-induced scrubbing process. [20, 29]. The damages were less observed in Fig. 3(d) and Fig. 3(e) of the precursor graphite and the commercial graphene, of which the ratios of I<sub>D</sub>/I<sub>G</sub> values were smaller.

### 3.3. Experiments with Exfoliated Graphite Samples

#### 3.3.1. Sedimentation experiment

The absorbance of the suspension of exfoliated graphite in 1%wt/vol SDS solution was measured covering a range of the wavelength between 330 and 600 nm and the results of all samples were shown in Fig. 4.

It could be observed from Fig. 4 that in the beginning of the sedimentation, the absorbance values of the suspensions of the sample G-7 and the commercial graphene were the same which was higher than those of the sample G-1, graphite and the sample G-6. The order was changed to G-7, G-1, the commercial graphene, graphite and closely followed by G-6 at the settling time of 20 min. This indicated that, among the exfoliated

samples, G-7 showed the best degree of dispersion followed by G-1 and G-6, which could be attributable to both the smaller sizes in two dimensions (length and width) as well as possibly fewer layer (thickness) of the G-7 product. It is better-dispersed than the commercial graphene after 20 min of sedimentation.

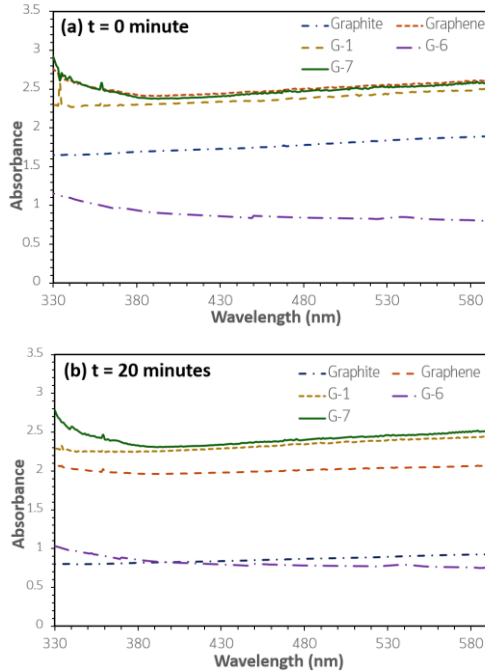


Fig. 4. The absorbance spectra of all suspensions were shown at the wavelength of 330 – 600 nm at (a)  $t = 0$  min and (b)  $t = 20$  min.

Theoretically, during sedimentation of particles, each particle is under the effect of various forces which are the weight of the particles, the buoyant force and the drag force (friction force) between the particle and the liquid. Initially, the particle settles with a resultant acceleration which is decreased along the settling time. Finally, the particle settles with a constant velocity called settling velocity,  $u_s$ , which could be determined from the equation of force balance as shown in Eq. (12).

$$u_s = \sqrt{\frac{2g(\rho_s - \rho)m}{A_p \rho_s C_D \rho}} \quad (12)$$

Here,  $\rho_s$  and  $\rho$  are the densities of solid particle and liquid, respectively.  $A_p$  is the projected area, to which the flow is directed.  $m$  is the mass of the particle and  $g$  is the gravitational acceleration.  $C_D$  is the drag coefficient which is a function of Reynolds number ( $Re = 4\rho Lu_s / \mu$ , where  $L$  is the nominal size of particle and  $\mu$  is the viscosity of the liquid). Because the exfoliated graphite could be considered fine particles, their settling was assumed in the range of a low  $Re$ , in which  $C_D = 24 / Re$ .

If graphite or few-layer graphene was assumed a particle having the size  $L_s \times W_s \times t_s$ , where  $L_s$  is the length,

$W_s$  is the width and  $t_s$  is the thickness of the solid particle. Then, the mass,  $m$  is  $\rho_s L_s W_s t_s$  and  $A_p$  is either  $L_s W_s$  or  $L_s t_s$ , or  $W_s t_s$ , depending on the side of the particle turning downward while settling. Replacing  $C_d$ ,  $m$  and  $A_p$  in Eq. (12), one of the possible equations is

$$u_s = \frac{g(\rho_s - \rho)(L_s t_s)}{3\mu} \quad (13)$$

Evidently, the settling velocity, which could affect the absorbance of the suspension, depends on the size of the particle as discussed earlier. It is interesting to check the order of magnitude of the settling velocity of graphene. The density of graphite or graphene is in the range of 2.09-2.27 kg/m<sup>3</sup> [30]. The density and viscosity of water at 25°C is 997 kg/m<sup>3</sup> and 8.90x10<sup>-4</sup> Pa·s, respectively [31]. The size of the commercial graphene was given by the company as 5  $\mu$ m in length and 6-8 nm in thickness. The settling velocity of graphene could be 1.52x10<sup>-4</sup> cm/s. At 20 min, the traveling distance should be about 0.18 cm which is very small.

The absorbance values at various times were collected up to 20 min so the turbidity percentages of all samples could be determined according to Eq. (3). The results of turbidity percentages were shown in Fig. 5.

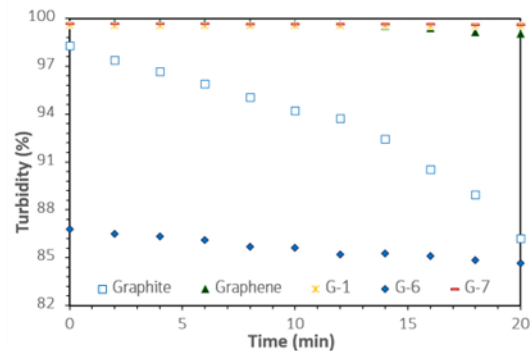


Fig. 5. The turbidity percentages of all samples along the settling time up to 20 min.

It could be simply assumed that the suspension turbidity ( $T$ ) is proportional to the number of settling particles ( $N$ ) so

$$\frac{dT}{dN} = k_T \quad (14)$$

where  $k_T$  is a constant. In addition, the change of the number of settling particles ( $N$ ) in a settling length ( $L$ ) could be considered proportional to the settling velocity so

$$\frac{dN}{dt} = -k_v u_s \quad (15)$$

Therefore, the change of turbidity over the settling time could be derived as

$$\frac{dT}{dt} = \left( \frac{dT}{dN} \right) \left( \frac{dN}{dt} \right) = (k_T)(-k_U u_t) \quad (16)$$

Equation (16) shows that the change of suspension turbidity over time is dependent on the settling velocity. Next, inserting Eq. (14) and Eq. (15) in Eq. (16), the relation for the change of suspension turbidity over the settling time was obtained from Eq. (17).

$$\frac{dT}{dt} = - \frac{k_T k_U g (\rho_s - \rho) (L_s t_s)}{12 \mu} \quad (17)$$

Therefore, the change of suspension turbidity over time depends on the size ( $L_s$ ) as well as the number of layers (thickness,  $t_s$ ) of the exfoliated graphite samples. If the particles were smaller, the sedimentation is slower and then the suspension would be more turbid for a long time. As seen from Fig. 5, the turbidity of the sample in the order of high to low is from the sample G-7, G-1, the commercial graphene, graphite and G-6. Additionally, considering the slope of the graph in Fig. 5, it was seen that the highest one is from graphite followed by G-6 of which the initial turbidity was the lowest, followed by the commercial graphene, G-1 and G-7, indicating that the size of G-7 was the smallest. The results of G-6 were unexpected. This could be from the aggregation of particles in the beginning of the sedimentation.

### 3.3.2. Adsorption experiment

Adsorption is a physicochemical process describing the separation of molecules from the gas or liquid phase to the adsorbent surface [32]. In this study, the samples G-1, G-6 and G-7 were experimented along with the precursor graphite and the commercial graphene. The concentration of MB was varied from 1.25 to 9 ppm while the amount of the adsorbate was fixed. For the adsorption kinetics study, the results of the experiment using 9 ppm MB solution were shown as an example in Fig. 6, while for the adsorption equilibrium study, the results of the experiment using the sample G-6 was displayed as an example in Fig. 7.

Figure 6 showed the plot of experimental results (dots) along with the predicted values (lines) from the pseudo-first-order model represented by Eq. (7) and pseudo-second-order model represented by Eq. (9). The parameters of the pseudo-first-order and pseudo-second-order kinetics equations were shown in Table 3.

As seen in Fig. 6(a), the correlation between the experimental and predicted values was not as good as that shown in Fig. 6(b), which could be confirmed by the value of  $R^2$  in Table 3. Those of the pseudo-first-order fittings were much less than 0.9 in all experiments so the pseudo-first-order model could not be used to explain the kinetics [32]. On the other hand, those of the pseudo-second-

order fittings in all, except for one, experiments were greater than 0.9 so the pseudo-second-order model could be adopted to explain the adsorption kinetics in this study. As the values of  $R^2$  were greater than 0.9, the predicted values of the equilibrium adsorption capacity,  $q_e$ , were also close to the experimental values at the longest adsorption time of 120 min. For each adsorbent sample, the equilibrium adsorption capacity increased with the initial concentration of MB solution, indicating that up to 9 ppm, the surfaces of all samples could still accommodate more adsorbate molecules from the liquid phase. Comparing all adsorbent samples, at the initial MB concentration at 1.25 ppm,  $q_e$  of all samples were not much different while at a higher MB concentration (from 2.5 to 9 ppm), the highest value of  $q_e$  was obtained from the sample G-7 which was also greater than that from the commercial graphene. Compared among all exfoliated graphite products, the sample G-7 gave the highest value of  $q_e$ , followed by the samples G-1 and G-6. Interestingly, this finding was consistent with the sedimentation results so it is possible that the smaller size and fewer layers of the exfoliated graphite could result in higher degree of dispersion and this in turn could result in better adsorption capacity. The smaller size could be actually resulted from the breakage of sample sheets, which should not affect the total surface area of the sample much. Because, the adsorption capacity depends greatly on the surface area of the adsorbents, these sets of adsorption results indicated the increase of total surface area after exfoliation to fewer layer sheets.

The changes of adsorption capacity ( $q_t$ ) and adsorption percentage along the adsorption time were also shown in Fig. 6(c) and Fig. 6(d), respectively. It was evidently observed that the adsorption capacity could reach the equilibrium or almost close to equilibrium in less than 20 min. The fluctuation of the adsorption capacity in the first hour of adsorption was observed for the samples G-1, G-6 and graphite, probably attributed to the bad dispersion of the samples in MB solution and weak attractive forces between MB molecules and the layers of the graphite, unlike the strong attractive force when adsorbed inside the micropores of activated carbon [33]. The values of  $k_2$  did not seem to show any obvious trend.

Langmuir and Freundlich isotherm models according to Eq. (10) and (11), respectively, were applied to fit the adsorption equilibrium results [34]. As an example, the results of the sample G-6 were shown in Fig. 7(a) and Fig. 7(b). The parameters of both isotherms for all adsorbents were reported in Table 4 along with the values of  $R^2$ . The parameter  $q_m$  in Langmuir adsorption isotherm represents the maximum adsorption capacity of methylene blue (MB) on the surface of the samples. The  $q_m$  values for G-1, G-6, G-7, the precursor graphite, and the commercial graphene were 31.45, 40.49, 38.02, 29.15 and 42.37 mg/g, respectively. Comparing these values with ones of  $q_e$  when using the initial MB concentration of 9 ppm which were 33.44, 32.90, 54.00, 38.02 and 42.19 mg/g, it was found that not all values of  $q_m$  were possible.

Table 3. The obtained values of  $k_1$ ,  $k_2$ ,  $q_e$  and  $R^2$  of pseudo-first-order and pseudo-second-order kinetics models.

Sample	MB Concentration	Pseudo-first-order			Pseudo-second-order		
		$k_1$ ( $\text{min}^{-1}$ )	$q_e$	$R^2$	$k_2$ ( $\text{g mg}^{-1} \text{min}^{-1}$ )	$q_e$	$R^2$
G-1	1.25	0.0127	2.96	0.5370	0.2016	7.67	0.9927
	2.5	0.0385	5.55	0.6855	0.0198	13.55	0.9959
	3	0.0029	3.23	0.5166	0.0318	15.82	0.9990
	5	0.0246	6.18	0.6373	0.0112	20.04	0.9957
	9	0.0076	24.21	0.5883	0.0173	33.44	0.9911
G-6	1.25	0.0119	3.60	0.6449	0.0373	7.62	0.9840
	2.5	0.0287	4.77	0.8225	0.0221	15.28	0.9992
	3	0.0308	6.92	0.8776	0.0108	17.15	0.9983
	5	0.0071	12.15	0.5177	0.0354	20.45	0.9926
	9	0.0112	30.80	0.6582	0.0016	32.89	0.8398
G-7	1.25	0.0186	5.57	0.5340	0.0556	8.44	0.9542
	2.5	0.0405	4.29	0.2689	0.0298	20.24	0.9997
	3	0.0324	7.93	0.4322	0.0107	22.92	0.9982
	5	0.0321	15.21	0.6599	0.0053	36.72	0.9964
	9	0.0311	20.60	0.6565	0.0047	54.00	0.9945
Graphite	1.25	0.0325	3.23	0.6571	0.0599	8.71	0.9965
	2.5	0.0314	5.97	0.6736	0.0522	10.01	0.9891
	3	0.0177	4.20	0.6633	0.0201	13.05	0.9888
	5	0.0144	5.19	0.6644	0.0200	10.99	0.9602
	9	0.0171	6.29	0.5176	0.1134	38.02	0.9993
Graphene	1.25	0.0167	3.74	0.7144	0.0121	8.76	0.9892
	2.5	0.0236	6.60	0.8646	0.0069	17.24	0.9846
	3	0.0208	6.18	0.5693	0.0063	20.24	0.9849
	5	0.0182	8.28	0.7266	0.0041	27.40	0.9602
	9	0.0215	10.18	0.5494	0.0174	42.19	0.9972

Table 4. Langmuir and Freundlich isotherm parameters for the MB adsorption of different samples.

Sample	Langmuir			Freundlich		
	$q_m$ ( $\text{mg/g}$ )	$K_L$ ( $\text{L/mg}$ )	$R^2$	$K_F$ ( $\text{mg/g}$ )	$1/n$	$R^2$
G-1	31.45	0.93	0.9775	14.10	0.53	0.9954
G-6	40.49	0.58	0.9655	13.62	0.51	0.9125
G-7	38.02	0.91	0.9046	34.25	0.32	0.9730
Graphite	29.15	1.39	0.8842	15.36	0.54	0.8857
Graphene	42.37	2.46	0.9316	25.89	0.34	0.9827

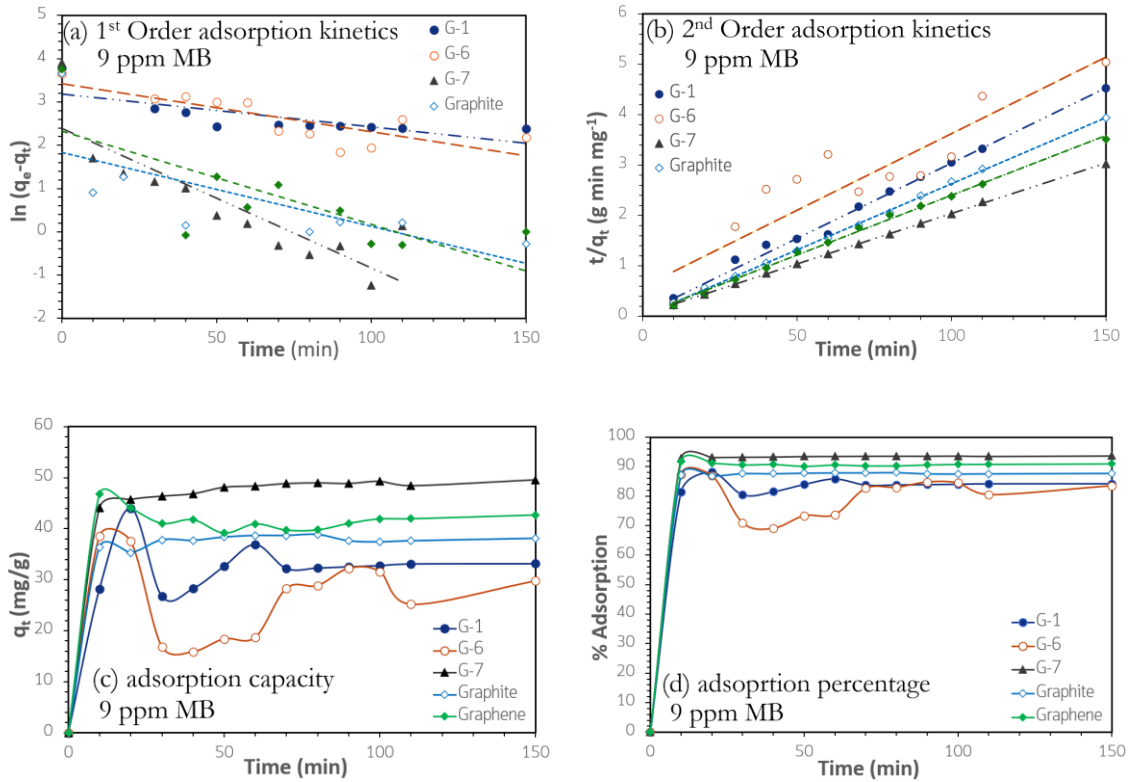


Fig. 6. The fittings of (a) pseudo-1<sup>st</sup> order and (b) pseudo-2<sup>nd</sup> order kinetics models together with the results of (c) the MB adsorption capacity and (d) the adsorption percentage along the adsorption time.

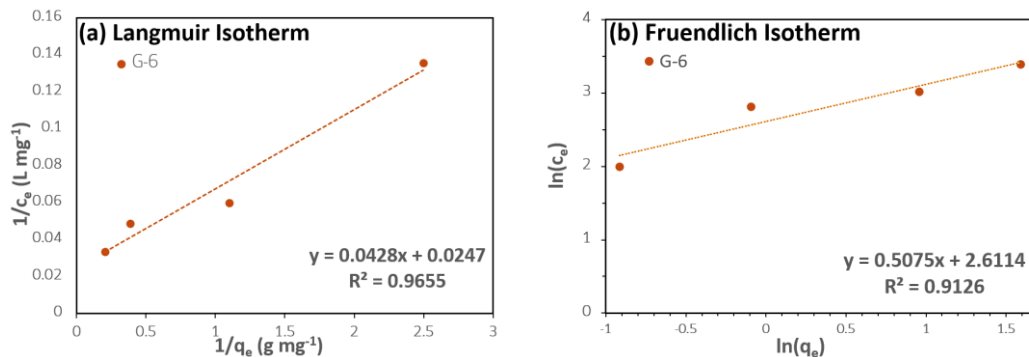


Fig. 7. The equilibrium adsorption results were shown fitted with (a) Langmuir isotherm and (b) Freundlich isotherm.

Therefore, the Freundlich isotherm was better in this study. The parameter  $K_F$  is the Freundlich constant which is related to adsorption capacity of the adsorbent (mg/g). The index  $1/n$  is related to adsorption intensity indicating whether the adsorption is favorable. Table 5 also listed the relevant parameters derived from Freundlich isotherm model. The values of  $K_F$  of the sample G-7 was the highest followed by those of the commercial graphene, graphite, G-1 and G-6, showing the same order as for the values of  $q_e$  when using the initial MB concentration of 9 ppm, the highest concentration applied in this study. Additionally, if the value of  $n$  is greater than 1, the adsorption of molecules on top of each other is considered favorable [32]. As shown, all adsorbents gave values of  $n$  greater than

#### 4. Conclusions

In this research, the serum from SNRL which still contained the left-over ammonia was used as the exfoliating medium in liquid exfoliation of graphite. Multi-step of exfoliation was applied and the overall yield could be increased but it was still not attractive. However, this work, based on the Raman spectroscopy results, showed that various quality levels of exfoliated graphite products could be obtained in the multi-step exfoliation. After exfoliation, the values of  $I_{2D}/I_G$  ratio of some foliated samples were higher than that of the precursor graphite and some were also higher than that of the commercial graphene. Three were chosen, ones with  $I_{2D}/I_G$  greater

than (G1), close to (G6) and less (G7) than that of the Commercial graphene.

In the sedimentation experiment, the exfoliated graphite samples, G-1 and G-7, could be suspended in the water better than the precursor graphite and the sample G-7 was even better than the commercial graphene. Similarly, in the adsorption experiment, the samples G-1 and G-7 could adsorb MB with higher adsorption capacity than the precursor graphite and the sample G-7 could do even better than the commercial graphene. The sample G-6 in both experiments showed worse results than those of the precursor graphite, possibly from the aggregation of the sample during preparation.

Therefore, it seemed consistent that the quality of graphene, such as dispersion in water and adsorption capacity, depended on the degree of exfoliation which was roughly related to the  $I_{2D}/I_G$  ratio. This work confirmed that the quality of the exfoliated samples using the serum from SNRL could be in the same or even higher level than the commercial graphene but the yield was still low, which could be investigated further in the future. Two possibilities could be tested. One is that lowering the ratio of the graphite mass and the exfoliating medium volume and the other is separation of the graphite population based on the its size first and different condition in the exfoliation process is applied to different sample.

## Acknowledgement

The authors would like to acknowledge the Department of Chemical Engineering and the Faculty of Engineering, Thammasat School of Engineering, Thammasat University for the financial support of this work. Natchanon Jirasitthanit is also grateful to the Faculty of Engineering for the Graduate Scholarship under the contract number of n.09/2564.

## References

- [1] P. Danwanichakul, T. Suwattharak, C. Suwanvisith, and D. Danwanichakul, "The role of ammonia in synthesis of silver nanoparticles in skim natural rubber latex," *Journal of Nanoscience*, vol. 2016, 2016, Art. no. 7258313. [Online]. Available: <http://dx.doi.org/10.1155/2016/7258313>
- [2] P. Danwanichakul and B. Than-ardna, "Permeation of salicylic acid through skim natural rubber films," *Industrial Crops and Products*, vol. 122, pp. 166-173, 2018.
- [3] P. Danwanichakul, W. Pohom, and J. Yingsampancharoen, "l-Quebrachitol from acidic serum obtained after rubber coagulation of skim natural rubber latex," *Industrial Crops and Products*, vol. 137, pp. 157-161, 2019.
- [4] P. Danwanichakul, R. Werathirachot, C. Kongkaew, and S. Loykulnant, "Coagulation of skim natural rubber latex using chitosan or polyacrylamide as an alternative to sulfuric acid," *European Journal of Scientific Research*, vol. 62, no. 4, pp. 537-547, 2011.
- [5] T. Suwattharak, B. Than-ardna, D. Danwanichakul, and P. Danwanichakul, "Synthesis of silver nanoparticles in skim natural rubber latex at room temperature," *Materials Letters*, vol. 168, pp. 31-35, 2016.
- [6] P. Pongsanon and P. Danwanichakul, "Synthesis of gold nanoparticles using serum from skim natural rubber latex: The effect of remaining coagulants," (in Thai) *Thai Science and Technology Journal (TSTJ)*, vol. 28, no. 4, pp. 596-606, 2020.
- [7] L. Chetia, D. Kalita, and G. Ahmed, "Synthesis of Ag nanoparticles using diatom cells for ammonia sensing," *Sensing and Bio-Sensing Research*, vol. 16, pp. 55-61, 2017.
- [8] M. Srikaew and S. Saengsuwan, "Miraculous material graphene: Synthesis strategies identification development properties and application," *Journal of Science and Technology, Ubon Ratchathani University*, vol. 22, no. 2, pp. 39-49, 2020.
- [9] R. S. Edwards and K. S. Coleman, "Graphene synthesis: Relationship to applications," *Nanoscale*, vol. 5, no. 1, pp. 38-51, 2013.
- [10] W. S. Hummers Jr. and R. E. Offeman, "Preparation of graphitic oxide," *Journal of the American Chemical Society*, vol. 80, no. 6, pp. 1339-1339, 1958.
- [11] E. Kusriani, I. Ramadhani, M. I. Alhamid, N. Y. Voo, and A. Usman, "Synthesis and adsorption performance of graphene oxide-polyurethane sponge for oil-water separation," *Engineering Journal*, vol. 26, no. 1, pp. 1-9, 2022.
- [12] F. T. Thema, M. J. Moloto, E. D. Dikio, N. N. Nyangiwe, L. Kotsedi, M. Maaza, and M. Khenfouch, "Synthesis and characterization of graphene thin films by chemical reduction of exfoliated and intercalated graphite oxide," *Journal of Chemistry*, vol. 2013, 2013, Art. no. 150536. [Online]. Available: <https://doi.org/10.1155/2013/150536>
- [13] M. Rasoulzadehzali and H. Namazi, "Facile preparation of antibacterial chitosan/graphene oxide-Ag bio-nanocomposite hydrogel beads for controlled release of doxorubicin," *International Journal of Biological Macromolecules*, vol. 116, pp. 54-63, 2018.
- [14] N. I. Zaaba, K. L. Foo, U. Hashim, S. J. Tan, W. W. Liu, and C. H. Voon, "Synthesis of graphene oxide using modified hummers method: Solvent influence," *Procedia Engineering*, vol. 184, pp. 469-477, 2017.
- [15] S. R. B. Nazri, W. W. Liu, C. S. Khe, N. M. S. Hidayah, Y. P. Teoh, C. H. Voon, H. C. Lee, and P. Y. P. Adelyn, "Synthesis, characterization and study of graphene oxide," in *AIP Conference Proceedings*, 2018, vol. 2045, p. 020033,
- [16] L. Hu, Q. Cheng, D. Chen, M. Ma, and K. Wu, "Liquid-phase exfoliated graphene as highly-

- sensitive sensor for simultaneous determination of endocrine disruptors: Diethylstilbestrol and estradiol,” *Journal of Hazardous Materials*, vol. 283, pp. 157-163, 2015.
- [17] A. Hadi, J. Zahirifar, J. Karimi-Sabet, and A. Dastbaz, “Graphene nanosheets preparation using magnetic nanoparticle assisted liquid phase exfoliation of graphite: the coupled effect of ultrasound and wedging nanoparticles,” *Ultrasonics Sonochemistry*, vol. 44, pp. 204-214, 2018.
- [18] B. Liang, K. Liu, P. Liu, L. Qian, G. Zhao, W. Pan, and C. Chen, “Organic salt-assisted liquid-phase shear exfoliation of expanded graphite into graphene nanosheets,” *Journal of Materiomics*, vol. 7, no. 6, pp. 1181-1189, 2021.
- [19] A. V. Tyurnina, J. A. Morton, T. Subroto, M. Khavari, B. Maciejewska, J. Mi, N. Grobert, K. Porfyrakis, I. Tzanakis, and D. G. Eskin, “Environment friendly dual-frequency ultrasonic exfoliation of few-layer graphene,” *Carbon*, vol. 185, pp. 536-545, 2021.
- [20] H. Ma, Z. Shen, M. Yi, S. Ben, S. Liang, L. Liu, Y. Zhang, X. Zhang, and S. Ma, “Direct exfoliation of graphite in water with addition of ammonia solution,” *Journal of Colloid and Interface Science*, vol. 503, pp. 68-75, 2017.
- [21] D. Hou, Q. Liu, X. Wang, Z. Qiao, Y. Wu, B. Xu, and S. Ding, “Urea-assisted liquid-phase exfoliation of natural graphite into few-layer graphene,” *Chemical Physics Letters*, vol. 700, pp. 108-113, 2018.
- [22] W. Nabnean and N. Jirasitthanit, “Exfoliation of graphite using natural substances,” senior project, AE, Thammasat University, Pathum Thani, PTE, 2020.
- [23] V. Khetsophon, “Look at the direction of Thai rubber in year 62, rising or falling?,” Thai Latex Association, Hat Yai, Songkhla, 2019.
- [24] P. Danwanichakul, D. Dechojarasri, S. Meesumrit, and S. Swangwareesakul, “Influence of sulfur-crosslinking in vulcanized rubber chips on mercury (II) removal from contaminated water,” *Journal of Hazardous Materials*, vol. 154, no. 1-3, pp. 1-8, 2008.
- [25] N. Jahan, H. Roy, A. H. Reaz, S. Arshi, E. Rahman, S. H. Firoz, and M. S. Islam, “A comparative study on sorption behavior of graphene oxide and reduced graphene oxide towards methylene blue,” *Case Studies in Chemical and Environmental Engineering*, vol. 6, p. 100239, 2022.
- [26] L. Zhao, P. Tang, Q. Sun, S. Zhang, Z. Suo, H. Yang, X. Laio, and H. Li, “Fabrication of carboxymethyl functionalized  $\beta$ -cyclodextrin-modified graphene oxide for efficient removal of methylene blue,” *Arabian Journal of Chemistry*, vol. 13, no. 9, pp. 7020-7031, 2020.
- [27] Y. Wang, J. Pan, Y. Li, P. Zhang, M. Li, H. Zheng, X. Zhang, H. Li, and Q. Du, “Methylene blue adsorption by activated carbon, nickel alginate/activated carbon aerogel, and nickel alginate/graphene oxide aerogel: A comparison study,” *Journal of Materials Research and Technology*, vol. 9, no. 6, pp. 12443-12460, 2020.
- [28] C. V. Gomez, M. Guevara, T. Tene, L. Villamagua, G. T. Usca, F. Maldonado, C. Tapia, A. Cataldo, S. Bellucci, and L.S. Caputi, “The liquid exfoliation of graphene in polar solvents,” *Applied Surface Science*, vol. 546, p. 149046, 2021.
- [29] R. Navik, Y. Gai, W. Wang, and Y. Zhao, “Curcumin-assisted ultrasound exfoliation of graphite to graphene in ethanol,” *Ultrasonics Sonochemistry*, vol. 48, pp. 96-102, 2018.
- [30] H. O. Pierson, *Handbook of Carbon, Graphite, Diamonds and Fullerenes: Processing, Properties and Applications*. William Andrew, 2012, pp. 51-52, 2012.
- [31] Engineers Edge, “Water-density viscosity specific weight,” Engineers’ Edge, 2000. Accessed: 21 May 2019. [Online]. Available: [https://www.engineersedge.com/physics/water\\_density\\_viscosity\\_specific\\_weight\\_13146.htm](https://www.engineersedge.com/physics/water_density_viscosity_specific_weight_13146.htm)
- [32] X. L. Wu, Y. Shi, S. Zhong, H. Lin, and J. R. Chen, “Facile synthesis of Fe<sub>3</sub>O<sub>4</sub>-graphene@ mesoporous SiO<sub>2</sub> nanocomposites for efficient removal of Methylene Blue,” *Applied Surface Science*, vol. 378, pp. 80-86, 2016.
- [33] D. Ramutshatsha-Makhwedzha, A. Mavhungu, M.L. Moropeng, and R. Mbaya, “Activated carbon derived from waste orange and lemon peels for the adsorption of methyl orange and methylene blue dyes from wastewater,” *Heliyon*, vol. 8, no. 8, p. e09930, 2022.
- [34] Z. Wang, M. Gao, X. Li, J. Ning, Z. Zhou, and G. Li, “Efficient adsorption of methylene blue from aqueous solution by graphene oxide modified persimmon tannins,” *Materials Science and Engineering: C*, vol. 108, p. 110196, 2020.



**Natchanon Jirasitthanit** received the B.Eng degree in chemical engineering from Thammasat University, Pathumthani, Thailand, in 2020 and is currently a master's student in the Department of Chemical engineering, Faculty of Engineering, Thammasat University. He had training at Bayer Thai Company Limited during the summer of 2021. After finishing his B.Eng degree, he got a scholarship from the faculty to pursue his master's study. His research interest is the green synthesis of nanomaterials and their applications.



**Panu Danwanichakul** received the B.Eng degree in chemical engineering from Chulalongkorn University, Thailand, in 1997, M.Eng. degree in chemical engineering from the University of Delaware, Newark, DE, in 1999 and the Ph.D. degree in chemical engineering from the University of Pennsylvania, Philadelphia, PA, in 2003.

Since 2003, he has worked at the Department of Chemical Engineering, Faculty of Engineering, Thammasat University, Pathumthani, Thailand and since 2008, he has been an associate professor at the department and used to serve as Associate Dean for Research and Graduate Studies, Head of the department and the Director of Graduate Studies at the department. His research interests include nanotechnology, statistical thermodynamics and molecular simulations.

Dr. Danwanichakul was a recipient of Best Teaching Award for the Field of Science and Technology from Thammasat University in 2006, Best Paper Award in IAENG Transactions on Engineering Technologies in 2008, Dissertation Award from National Research Council of Thailand in 2009 and Outstanding Research Award for the Field of Science and Technology from Thammasat University in 2010.